### An Efficient Pipeline for Biophysical Modeling of Neurons

Nathaniel Opsal, Pete Canfield, Tyler Banks, and Satish S. Nair, Senior Member, IEEE

Abstract— Automation of the process of developing biophysical conductance-based neuronal models involves the selection of numerous interacting parameters, making the overall process computationally intensive, complex, and often intractable. A recently reported insight about the possible grouping of currents into distinct biophysical modules associated with specific neurocomputational properties also simplifies the process of automated selection of parameters. The present paper adds a new current module to the previous report to design spike frequency adaptation and bursting characteristics, based on user specifications. We then show how our proposed grouping of currents into modules facilitates the development of a pipeline that automates the biophysical modeling of single neurons that exhibit multiple neurocomputational properties. The software will be made available for public download via our site cyneuro.org.

#### I. Introduction

Computational models of single neurons utilize a variety of formulations depending on the application. One such formulation, biophysical conductance-based model can provide improved realism in network models when investigating phenomena such as neuronal oscillations. Present single cell models have compartments varying from one in reduced order cells to over 1000 in morphologically complex cell models. Large neuronal network models typically use reduced order models of single cells to limit both computational overheads and parametric uncertainties [1]. However, in such cases, it is important that the reduced order model neuron possess key neurocomputational properties including passive properties, current injection responses as well as possibly complex oscillatory dynamics. We had previously hypothesized and successfully tested the hypothesis that in a single neuron, sets of currents organized in modules might be responsible for neurocomputational properties such as passive properties (resting membrane potential (RMP), time constant and input resistance), subthreshold oscillations, and spike waveforms [2]. Furthermore, the hypothesis naturally suggested an approach, termed the 'segregation method', that was shown to facilitate the selection of single cell model parameters and to simplify the overall design. Such a simplification in design facilitates automation of the process of optimizing the numerous parameters associated with Hodgkin-Huxley formulations in the biophysical conductance-based models of single neurons.

Here, as a first contribution, we first extend the biophysical-based segregation method [2] to also include another neurocomputational propertfy of spike frequency adaptation and bursting. As a second contribution, we propose a pipeline to automate the design process using a recently

reported machine learning scheme that includes Bayesian and fully connected neural network modules (simulation-based inference, sbi; [3]). We illustrate the proposed scheme using an example of a pyramidal neuron in the CA3 region of the hippocampus that responds to stimuli with a rapidly adaptive burst waveform that then reduces to tonic spiking or to a continuously bursting phenotype, both of which are commonly found neural signatures [4]. We then show that such a waveform output of CA3 neurons plays an important role in the generation of theta oscillations in the model hippocampal network. We will make the automated pipeline for modeling publicly accessible to the neuroscience community to facilitate designing single neuron models.

#### II. METHOD

Models of single neurons were developed using experimental parameters from our collaborators and the literature [2], and implemented using the NEURON 7.4 simulator [5] with a fixed time step of 25 µs. We first describe a brief overview of the mathematical underpinnings of both single cell dynamics and of the segregation approach [2].

### Mathematical equations for voltage-dependent ionic currents.

The dynamics for each compartment (soma or dendrite) followed the Hodgkin-Huxley formulation [4] in eqn. 1,

$$\frac{C_m dV_s}{dt} = -g_L eak(V_s - E_{Leak}) - g_c(V_s - V_d) - \sum_{cur,s} I_{cur,s}^{int} - \sum_{cur,s} I_{cur,s}^{syn} + I_{inj}$$
 (1)

where  $V_s/V_d$  are the somatic/dendritic membrane potential (mV),  $I_{cur,s}^{int}$  and  $I_{cur,s}^{syn}$  are the intrinsic and synaptic currents in the soma,  $I_{inj}$  is the electrode current applied to the soma,  $C_m$  is the membrane capacitance,  $g_{Leak}$  is the conductance of the leak channel, and  $g_c$  is the coupling conductance between the soma and the dendrite (similar term added for other dendrites connected to the soma). The intrinsic current  $I_{cur,s}^{int}$ , was modeled as  $I_{cur,s}^{int} = g_{cur} m^p h^q (V_s - E_{cur})$ , where  $g_{cur}$  is its maximal conductance, m its activation variable (with exponent p), h its inactivation variable (with exponent q), and  $E_{cur}$  its reversal potential (a similar equation is used for the synaptic current  $I_{cur,s}^{syn}$  but without m and h). The kinetic equation for each of the gating variables x (m or h) takes the form but without m and h. The kinetic equation for each of the gating variables x (m or h) takes the form

$$\frac{dx}{dt} = \frac{x_{\infty}(V, [Ca^{2+}]_i) - x}{\tau_X(V, [Ca^{2+}]_i)}$$
 (2) where  $x_{\infty}$  is the steady state gating voltage- and/or Ca<sup>2+</sup>-

dependent gating variable and  $\tau_x$  is the voltage- and/or Ca<sup>2+</sup>-

This research was supported in part by This research was supported in part by grants NIH MH122023 and NSF OAC-1730655 to SSN.

\*N Opsal, P Canfield, T Banks and SS Nair are with Electrical Engineering and Computer Science, University of Missouri, Columbia MO

65211 (corresponding author SSN phone: 573-882-2964; fax: 573-882-0397; e-mail: nairs@missouri.edu).

dependent time constant. The equation for the dendrite follows the same format with 's' and 'd' switching positions in eqn. 1. The procedure for selecting the channel currents and their model parameters are described next using an approach we proposed recently.

### Segregation hypothesis in single cell design.

The hypothesis states that distinct current modules implement neurocomputational properties, e.g., passive properties (Vrest, input resistance, tau) and spiking properties in cartoon form in Fig.1. In this case, leak, and the hyperpolarization-activated cation current H (passive module) are responsible for passive properties. Similarly, leak, transient sodium Nat, and delayed rectifier Kdr currents set the spiking properties for the spiking module. The activation functions are segregated to prevent overlap, i.e., the currents of each module start on the voltage axis only after the zone of action of the module to its left. Cut-off values for the gating variables were selected to be within reported ranges of v-half values [6]. Details related to the approach with additional modules can be found in [2].

# Design of the Nap-KM module as option 1 for adaptation/bursting properties.

To design the neurocomputational property of adaptation and bursting, we first add the transient sodium (Nap) and the M type potassium (KM) as a module (known to provide this property to neurons [6]) to the 'passive' and 'spiking' modules in Fig. 1. An example case hippocampal CA3 neuron with an adapting characteristic [7] is considered to illustrate the procedure. The neuron also has other spiking currents transient sodium (Nat), delayed rectifier potassium (Kdr), hyperpolarization-activated cation current (H) and leak currents, which are kept fixed here. The ranges for the adjustable parameters for Nap-KM modules of the CA3 neuron, based on biological reports, were as follows (units for g is mS/cm2 and for V1/s is mV): gNap – [1\*10-5, 0.005], gKM – [5\*10-6, 0.017], V<sub>1/2</sub> Nap - [-65, -35], V<sub>1/2</sub> KM - [-50, 0] [6].

# Design of the CaS-CaT-sAHP module as option 2 for adaptation/bursting properties.

A second option to implement adaptation and busting is the set of currents that include a low-threshold Ca2+ (CaS), high-threshold Ca2+ (CaT) and the calcium-activated potassium (sAHP) currents.

A different class of the same hippocampal CA3 neuron that exhibits the bursting characteristic [8] is considered for this option. Like the case above, the ranges for the parameters for this set of current were as follows (units for g is mS/cm2 and for V1/s is mV): gCaS - [1\*10<sup>-5</sup>, 0.017], gCaT- [1\*10<sup>-5</sup>, 0.017], gsAHP - [1\*10<sup>-5</sup>, 0.008], V $_{1/2}$  CaS - [-33], V $_{1/2}$  CaT - [-27.1].

#### III. RESULTS

The two options to model spike frequency adaptation and bursting into model neurons via the approach that groups currents into modules using a segregation approach is illustrated using an example case hippocampal neuron from our previous publication [9].

## Design of two current modules to implement spike frequency adaptation and bursting

<u>Nap-KM module</u>. This module adds the neurocomputational property of adaptation and bursting, depending on the parameters of the two currents. Both channels can be segregated up to  $\sim$ -60 mV in this model. Optimizing the

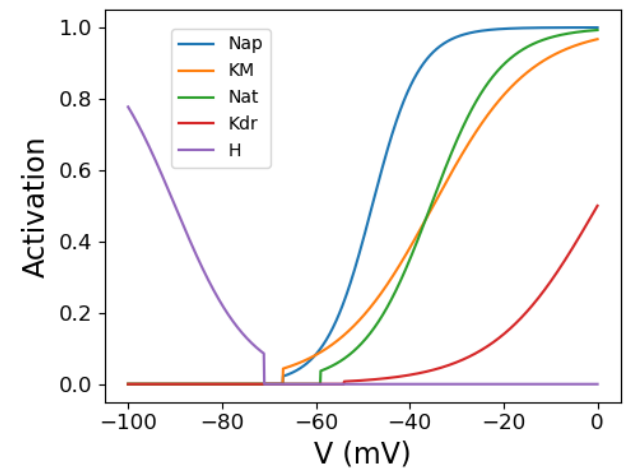
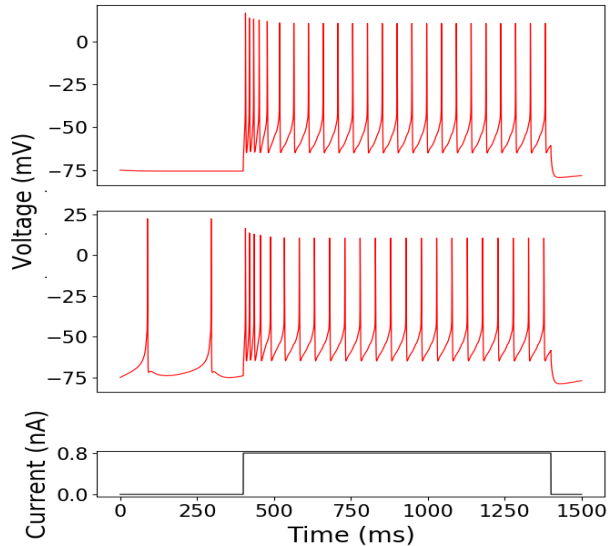


Figure 1. Example of segregation of into three modules – passive (H), adapting/bursting (Nap, KM) and Spiking (Nat, Kdr) modules in the example hippocampal CA3 cell.

parameters after implementing the segregation (Fig. 1) resulted in the following parameter set that provided the adapting characteristic shown in Fig. 2A that matches the biological current injection (Fig. 2C) response in [6] well: gNap = 0.0005, gKM = 0.017,  $V_{1/2}$  Nap = -48,  $V_{1/2}$  KM = 35.

Adaptation happens when KM current builds up enough to counteract the Nap current. The time constant of KM controls the duration of the initial high frequency of the adapting characteristic. On the other hand, increasing gKM and gNap together (~0.17 and 0.001, respectively) shuts off spiking and results in a bursting characteristic. Importantly,



Figures 2. CA3 Pyramidal cell response to current injection when segregated (2A, top) and unsegregated (2B, middle)

without such a segregation of the current modules, it was very difficult to hand-tune the parameters due to the interactions

between the currents. Such interaction effects resulted in changes to spiking properties affecting passive properties, and so on. This makes the tuning process very difficult, for both hand- and automated-tuning scenarios [2]. This neuron becomes an endogenous spiker if segregation is not implemented (Fig. 2B).

<u>CaS-CaT-sAHP module</u>: This second option to add adaptation/bursting involves three currents. CaS is segregated at -64 mV; CaT and sAHP remain unsegregated (Fig. 3A). The parameter set after implementing the segregation scheme (Fig. 3A) and tuning are as follows: gCaS =0.00425, gCaT =0.001, gsAHP = 0.005. These

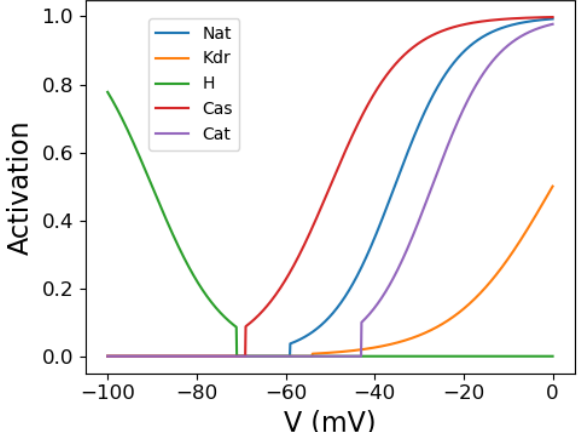


Figure 3A. Segregation of currents into three modules for the second option – passive (H), adapting/bursting (CaS, CaT and sAHP) and Spiking (Nat, Kdr) for example hippocampal CA3 cell.

resulted in a bursting profile. Without segregation, the CaS-CaT-sAHP module will offset Vrest by around 0.3mV. Eleak can be altered to account for this change; however, altering Eleak will result in a change in both inter-burst interval (IBI) and spikes per burst. Fixing this involves a time-consuming retuning of the cell which is less preferable compared to the alternative of segregating the CaS channel appropriately.

Bursting is controlled in this module by  $\tau_{sAHP}$  and  $\tau_{Ca\text{-pool}}$ .  $\tau_{sAHP}$  can be increased or decreased largely independently to increase or decrease, respectively, the number of spikes per burst. Similarly,  $\tau_{Ca\text{-pool}}$  can be increased or decreased almost independently to increase or decrease, respectively, the interbest interval.

Some interesting **neural dynamic characteristics** that we noted for the Nap-KM and CaS-CaT-sAHP modules were as follows (Fig. 3B): (i) the ranges of IBI for the Nap-KM module are set by the lower/higher biological ranges for the time constant of the KM current, of 46 ms and 120 ms, respectively. The maximum spike frequency was 125 Hz. (ii) For the CaS-CaT-sAHP module, the minimum IBI was 120 ms, set by the minimum time constant for the Ca2+ pool to permit sAHP to activate. Ranges were not found to set the maximum on the IBI in this case. The maximum spiking frequency for this module was 77 Hz, set by the competing effects of CaS that raised the membrane potential to allow for faster spiking but also simultaneously increases activation of sAHP activation that causes inhibition.

As an application of the segregation module proposed in our paper, we used a previously developed CA3 hippocampal network model to demonstrate the importance of high initial bursts in pyramidal cells for theta generation [10]. After substituting a bursting CA3 pyramidal cell (segregated), we found that a 15 Hz Poisson random spike train to the model Entorhinal Cortex resulted in a power spectral density (PSD) theta peak of of 1.2 \* 10<sup>4</sup> (spk/sec) <sup>2</sup>/Hz at a frequency of 5 Hz (Fig. 4). However, with a tonically spiking cell

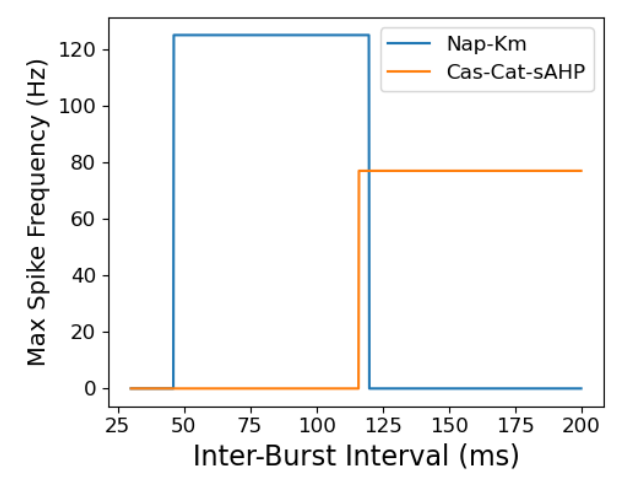


Figure 3B. Spike frequency and Inter-Burst Interval limits for both bursting Modules.

### Adaptive bursts are important to generate theta oscillations in a network of CA3 cells

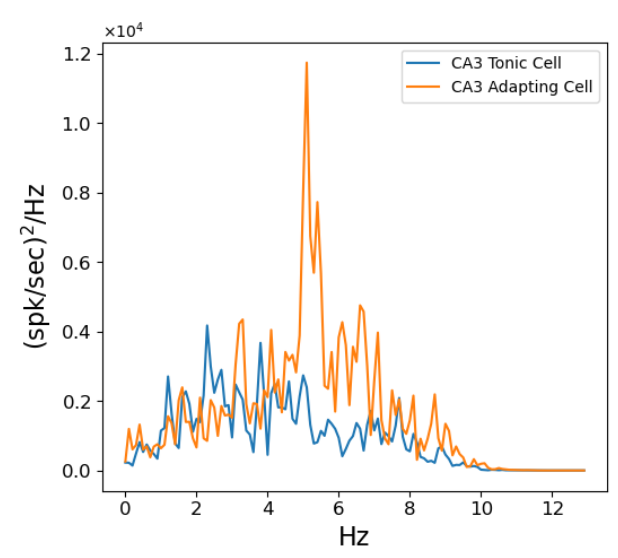


Figure 4. Power Spectral Density (PSD) using two different cell types for CA3 pyramidal cells in the network: a non-bursting tonic cell (original, blue) and a bursty cell (segregated, orange).

with same properties and FI curve (non-segregated case), theta power diminished considerably. PSD was calculated by partitioning spike times into 0.1 ms bins and calculating Fast Fourier Transform with a sliding window of 1024 ms and a 512 ms overlap. An insight/prediction of the model is that interactions with surrounding GABAergic interneurons via 'bursty' input from CA3 pyramidal cells produces theta power. Although the average frequency was matched when generating the two cases, we were not able to replicate the initial high frequency burst without segregation. This

suggests that the segregation technique may be critical for the design of cells with characteristics such as high initial bursts.

Automating the segregation process using machine learning As a first step in automating the segregation process using the Bayesian-based machine learning approach, we consider the CA3 cell with only the passive and spiking modules, i.e., the simple spiker case with only leak, H, Nat and Kdr channels. With the segregation scheme of Fig. 1, the validation performance was better and the posterior distribution was tighter, compared to the without segregation case. The next step will be to include the Nap-KM module independently to infer gNap, gKM and tau\_KM. Work is on-going to automate the pipeline of inferring the parameters of all the modules, i.e., passive, spiking and adapting modules simultaneously combining the segregation approach and simulation-based-inference (sbi;[3]) module.

#### IV. DISCUSSION AND CONCLUSION

Modeling single cells with multiple neurocomputational properties poses challenges at both theoretical and application levels. For instance, at the theoretical level it is not clear how the plethora of current channels coordinate to implement the seemingly distinct neural signatures. At the application level, procedures to select parameters including automated schemes, typically result in multiple parameter sets for the same solution (e.g., [11]). Moreover, automated schemes such as genetic algorithm searches (e.g., [12]) cannot provide mechanistic insights into the interactions among the channels.

### Distinct features of modules that implement spike-frequency adaptation and bursting.

The neurocomputational property of spike frequency adaptation and bursting was implemented via two known current modules, the distinct characteristics of which are highlighted by our approach. Parameters of the Nap-KM module were found to have several functional implications. Time constant  $\tau_{Nap}$  was found to be restricted to a small range suggesting that it might not vary much, and this time constant controls the rapid response of the burst. The initial high frequency of the burst was controlled by g<sub>Nap</sub>. The time constant  $\tau_{KM}$  controlled the duration of the burst and its conductance g<sub>KM</sub> controlled spikes per burst. In the twocurrent module,  $g_{\text{Nap}}$  and  $g_{\text{KM}}$  together controlled the frequency of the burst. And  $g_{KM}$  and  $\tau_{KM}$  together controlled the duration of the burst and the inter-burst interval. This made it difficult to independently set both burst duration and inter-burst interval with the Nap-KM module, suggesting that it may be better suited primarily for the adaptation characteristic. On the other hand, the CaS-CaT-sAHP module had additional degrees of freedom which made it possible to independently vary both burst duration and inter-burst interval. However, the Nap-KM module seems to allow for a faster burst spiking profile than what is possible with the CaS-CaT-sAHP module which may mean it is necessary in cells that display this characteristic.

Also, the analysis suggests **user tuning guidelines** for the Nap-KM module as follows: increasing  $\tau$ \_KM and gKM increases IBI; an increase in gNap increases spike frequency; number of spikes per burst can be increased by increasing

gNap, increasing  $\tau_KM$ , or decreasing gKM with the latter being the least effective. Similar guidelines for tuning the CaS-CaT-sAHP module are as follows: increasing  $\tau_Ca2$ +pool and  $\tau_SAHP$  increase IBI; spike frequency can be increased by gCaS; spikes per burst can be increased by decreasing gCaT or gsAHP, or by increase  $\tau_SAHP$ .

## Automated pipeline for developing biophysical models of single neurons

The segregation method with its lack of interaction among the various current modules makes the tuning process more efficient and facilitates automation via the machine learning package. Automation of the simple spiking module was shown in the Results section. Ongoing work focuses on extending the process to include the Nap-KM and CaS-CaT-sAHP modules separately. The final goal is to automate the entire pipeline including passive, spiking, adapting, and bursting modules, and make it available for public download via the site cyneuro.org.

#### REFERENCES

- Borgers C (2017) An introduction to modeling neuronal dynamics (Springer International Publishing).
- Alturki A, Feng F, Nair A, Guntu V, Nair SS (2016) Distinct current modules shape cellular dynamics in model neurons, Neuroscience 334, 309-331. PMC5086448.
- Gonçalves PJ, Lueckmann J-M, Deistler M, Nonnenmacher M, Öcal K, Bassetto G, Chintaluri C, Podlaski WF, Haddad SA, Vogels TP, Greenberg DS, Macke JH (2020) Training deep neural density estimators to identify mechanistic models of neural dynamics, eLife 9, e56261.
- Byrne JH, Roberts JL, Waxham MN (2014) From molecules to networks: An introduction to cellular and molecular neuroscience, 3rd edn (Elsevier).
- Carnevale N, Hines M (2006) The neuron book (UK: Cambridge University Press).
- Izhikevich (2007) Dynamical systems in neuroscience the geometry of excitability and bursting In Computational neuroscience (Cambridge, Mass., MIT Press).
- Sun Q, Sotayo A, Cazzulino AS, Snyder AM, Denny CA, Siegelbaum SA (2017) Proximodistal heterogeneity of hippocampal CA3 pyramidal neuron intrinsic properties, connectivity, and reactivation during memory recall, Neuron 95, 656-672.e653.
- Staff NP, Jung H-Y, Thiagarajan T, Yao M, Spruston N (2000) Resting and active properties of pyramidal neurons in subiculum and cal of rat hippocampus, J Neurophysiol 84, 2398-2408.
- Hummos A, Franklin Charles C, Nair Satish S (2014) Intrinsic mechanisms stabilize encoding and retrieval circuits differentially in a hippocampal network model, Hippocampus 24, 1430-1448. PMC24978936.
- Hummos A, Nair SS (2017) An integrative model of the intrinsic hippocampal theta rhythm, PLoS One 12, e0182648. PMC5546630.
- Prinz AA, Bucher D, Marder E (2004) Similar network activity from disparate circuit parameters, Nat Neurosci 7, 1345-1352.
- Achard P, De Schutter E (2006) Complex parameter landscape for a complex neuron model, PLoS Comput Biol 2, e94.